Fabrication of GC-r-GO-PAMAM (G3)-Pd electrode for electro-catalytic oxidation of formic acid

E. Murugan* and K. Kalpana

Department of Physical Chemistry, School of Chemical Sciences, University of Madras, Guindy Campus, Chennai, 600025, TamilNadu, India

*Corresponding author

DOI: 10.5185/amp.2018/815
www.vbripress.com/amp

Abstract

Graphene functionalized with Poly(amidoamine) dendrimer stabilized PdNPs (r-GO-PAMAM-Pd) composite was prepared through facile experimental routes and characterized by FT-IR, XRD, Raman, SEM and EDAX techniques. Initially, poly(amidoamine) generation 3 (PAMAM (G3)) dendrimer was functionalized on graphene oxide (GO) and the resulting matrix was loaded with PdNPs through stabilization and thus produced excellent conducting composite material. The electro-catalytic activity of this composite was inspected by coating on bare GCE and thus produced stable and efficient GC-r-GO-PAMAM (G3)-Pd electrode and this in turn demonstrated for the oxidation of formic acid (FA). The occurrence of the oxidation reaction was monitored by cyclic voltammetric (CV) and linear sweep voltammetric (LSV) techniques in 0.5 M H_2SO_4 medium at the potential window of -0.3 to 1.0 V vs. Ag/AgCl, v = 50 mVs^{-1}. The observed peak potential for the new electrode was located at 0.15V and compared with existing electrodes derived from different GO/Pd composites. The comparative results reveals that the newly designed electrode shown an excellent catalytic activity, more resistant to the surface poisoning and the anodic onset potential was more negative than the reported electrodes. This improved electro-catalytic performance are due to the contribution of synergetic effect of GO, dendrimer and PdNPs.

Keywords: Reduced graphene oxide, Poly(amidoamine), palladium nanoparticle, r-GO-PAMAM (G3)-Pd and FA.

Introduction

It is worthy to mention here that, increasing energy demands have stimulated intense research on alternative energy conversion and storage systems with high efficiency, low cost and environmental benignity [1]. Direct formic acid fuel cells (DFAFCs) have attracted great attention as a new generation of power sources with high operating power densities and low emissions [2−7]. Formic acid (FA) is an organic molecule, occurs naturally most notably in some ants. It is non-toxic, used as a food additive, inflammable and does not require special device for storage and transportation [8]. Moreover, DFAFCs have the potential to achieve better performance than direct methanol fuel cells (DMFCs). FA has two orders of magnitude smaller crossover flux through a nafion membrane than methanol allowing the use of highly concentrated fuel solutions in DFAFCs [9]. The DFAFCs can have higher power density than direct DMFCs. In addition, the electro-oxidation of FA occurs at a less positive potential than methanol [7]. Therefore, DFAFCs have many advantages over DMFCs and palladium has been emerging as a type of important catalyst in the development of industrial processes especially as an energy source and in fine chemical production and it has been a hot topic of interest in the FA oxidation because of their lower cost, higher abundance and greater resistance to CO as compared to Pt-based catalysts. Much effort has been devoted to development of simple and practical techniques to prepare Pd electro-catalysts with controllable micro/nanostructures and also enhanced performance for the DFAFCs applications [10−12]. In recent years, graphene has aroused significant interests as a flat monolayer of carbon atoms tightly packed into a two dimensional (2D) honeycomb lattice [13]. It has become one of the most exciting topics of research with potential applications in various fields such as solar cells, electronic devices, energy storage & conversion devices, biosciences and biotechnologies [14-15]. Graphene also is attractive solid support for catalysts due to its several excellent attributes, such as the huge theoretical specific surface area, excellent electronic conductivity, high chemical stability and low manufacturing cost makes graphene as the perfect catalyst support in fuel cells [16−18]. Although a few examples involving the synthesis of graphene/Pd hybrids have been demonstrated to date [19−20] some of the most critical issues yet to be improved are how to enhance the activity, durability and recyclability of the graphene/Pd catalysts for fuel cells and accordingly minimize the environmental contamination. To control the size and avoid the aggregation of Pd nanoparticles the catalyst stabilizers are very much essential to pursue higher active catalysts which should have ultrafine sizes, outstanding dispersibility and stability, such as surfactants [21] and polymers [22]. Although these molecules are stabilized the metal nanoparticles in better manner, but every template molecule has its own demerits. Dendrimers is a unique class of symmetrical and hyper branched polymer, which has an ability for high loading, high stability and production of controlled particle sizes and morphologies of nanoparticle catalyst [23]. Our earlier studies demonstrated that dendrimer stabilized metal nanoparticles [24]. Poly(amidoamine) (PAMAM) dendrimer is proved to be an attractive dendrimer which acts as good stabilizer and linker for the incorporation of metal nanoparticles on the surface of support materials for preparation of different catalyst. The functionalization of dendrimers on to the surface of graphene is a good strategy used for synthesis of new heterogeneous nanoparticle catalysts. In this study, we developed graphene supported poly(amidoamine) dendrimer stabilized Pd nanoparticles (r-GO-PAMAM-Pd) based conducting composite and used the same for fabrication of new electrode by coating the same on GCE. The activity of new electro-catalyst was demonstrated through FA electro-oxidation and the occurrence of the oxidation reaction was studied through cyclic voltammetric (CV) and linear sweep voltammetric (LSV) techniques.

Experimental

Materials

Powdered Graphite of particle size of 48mm, 99.95% purity, *N*-hydroxy succinimide, 1-Ethyl-3-[3-dimethylaminopropyl] carbodiimide, Poly(amidoamine) generation 3 (with 32 peripheral $–NH_2$ groups, PAMAM(G3)) and potassium tetrachloropalladate (II) was purchased from Sigma-Aldrich. Potassium permanganate, Sulphuric acid, Sodium nitrate and Sodium borohydride were obtained from SRL, India. Hydrogen peroxide, Hydrochloric acid, Hydrazine hydrate and Formic acid were purchased from Merck, India. Ethanol (Jiangsu Huaxi international trade Co ltd), De-ionized water (Merck), nafion 1 wt% (Sigma-Aldrich) were used without further purification. All reagents used were of analytical grade and all solutions were prepared with double distilled water.

Instrumentations

The Fourier transform infrared (FT-IR) spectra were recorded in the range of 4000 to 400 cm^{-1} on a Bruker Tensor-27 FTIR spectrophotometer with OPUS software. The Raman spectra were performed in a Witec Confocal Raman instrument (CRM200) with Ar ion laser (514.5 nm). The surface morphology study was performed using HITACHI SU 6600 scanning electron microscope (SEM). Ultra-sonication was done by Cole Palmer sonication bath using single distilled water as a dispersion medium with a frequency of 40 keV. X-ray powder diffraction (XRD) data were collected on PANalytical Instruments.

Electrochemical measurements

Electrochemical experiments were performed using a CHI1130A electrochemical work station (USA). A conventional three-electrode cell consisting of a glassy carbon electrode as a working electrode, Ag/AgCl with 3M KCl as a reference electrode and a platinum wire as a counter electrode with 20 mL working volume. The current was normalized to the apparent surface area of the glassy carbon electrode (0.0314 cm^2). The surface of the GCE was cleaned first mechanically by polishing with 0.05 and 1.0 μm alumina powder on a polishing cloth (Buehler) followed by sonication in DD water for 10 min. The electrode was then sonicated with absolute ethanol for about 5 min and rinsed thoroughly with double-distilled water. The solution containing electro catalyst samples
1.0 mg/mL in distilled water was prepared by ultrasonic agitation for 30 min and it was used as a stock solution. After the electrode surface was air dried, 5.0 µL of stock was drop cast onto the surface of the pre-treated GC electrode with a micropipette and then it was dried in air. The electrochemical measurements were performed in 0.5 M H_2SO_4 + 0.5 M formic acid solution.

Material synthesis

Synthesis of Graphene oxide

Graphene oxide (GO) was synthesized from natural graphite (48mm, 99.95% purity) powder by a modified Hummers method [25]. Briefly, 1 g of graphite, 1 g of $NaNO_3$ and 40 mL of H_2SO_4 were mixed and stirred in a three neck flask and then 6 g of $KMnO_4$ was slowly added. Once added, the solution was transferred to a 35 ± 1ºC water bath and stirred for about 1 h and then 80 mL distilled water was added and the solution was stirred for 30 min at temperature of 90ºC. Then, 150 mL distilled water was added and then 6 mL of H_2O_2 (30%) was also added slowly, turning the colour of the solution from dark brown to yellow. The warm solution was diluted with 1000 mL distilled water. The resulting mixture containing oxidized graphite was filtered and dried under vacuum and thus produced dark brown powder. This in turn characterised with FT-IR, XRD and Raman analyses.

Preparation of poly(amidoamine) grafted graphene oxide conjugate (GO-PAMAM (G3))

Initially, 50 mg graphene oxide was taken in a 100 mL round-bottom flask equipped with nitrogen protection and it was dispersed in 10 mL distilled water. Subsequently, 100 mg of 1-(3-dimethyl-amino-propyl)-3-ethyl carbodiimide (EDC) & 100 mg of N-hydroxy succinimide (NHS) were added to it and stirred for 30 min to activate the –COOH group of graphene oxide. The mixture was further treated with 100 mg of PAMAM (G3) dendrimer and vigorously stirred for 6 h. The excess reactants was removed under vacuum and then the resulted product was washed and dried under vacuum for 24 h and thus obtained GO-PAMAM (G3) conjugate. This in turn characterised with FT-IR and Raman analyses.

Synthesis of r-GO-PAMAM (G3)-Pd NPs composite

To deposit the Pd NPs onto the GO-PAMAM (G3) conjugate, 10 mg of r-GO-PAMAM (G3) conjugate was added to the 20 mL of de-ionized water. Then 24.48 mg of K_2PdCl_4 as Pd electro-catalyst precursor was dissolved in 10 mL of de-ionized water. Then, the catalyst precursor solution was added to the prepared GO-PAMAM (G3) conjugate solution and the mixture was stirred for 3 h at room temperature. A freshly prepared $NaBH_4$ solution was added dropwise into the above mixture and then the stirring was continued for another 16 h to make sure the complete reduction of Pd^{2+}. Finally, the resulting product was collected by centrifugation and washed five times then dried at 80ºC under vacuum for 12 h and thus obtains r-GO-PAMAM (G3)-Pd composite as a black colour powder (Scheme 1). This in turn was characterized through FT-IR, XRD, Raman, SEM and EDAX analyses. This is used for the fabrication of modified electrode for electro-catalysis reactions.

Fabrication of r-GO-PAMAM (G3)-Pd composite modified glassy carbon electrode for electro-catalytic oxidation of formic acid

In order to inspect the electro-catalytic activity of r-GO-PAMAM (G3)-Pd composite, glassy carbon electrode (GCE) was modified with r-GO-PAMAM (G3)-Pd composite and its electrochemical oxidation of FA was examined by CV and LSV. Prior to the fabrication, GCE was polished with finer grade alumina powders having the pore size of 0.05 and 0.3 individually and then electrode was purified by successive washing with ethanol and distilled water via sonication and the fresh electrode was dried at room temperature. Then 10 mg of the r-GO-PAMAM (G3)-Pd composite was dispersed in 10 mL water and it was used as a stock solution. Prior to the surface coating, the stock was sonicated for 5 min and from that stock solution, 5 µL of the suspension was withdrawn and drop-coated on the pre-treated GCE and allowed it to dry in ambient temperature and thus produced GC- r-GO-PAMAM (G3)-Pd electrode.

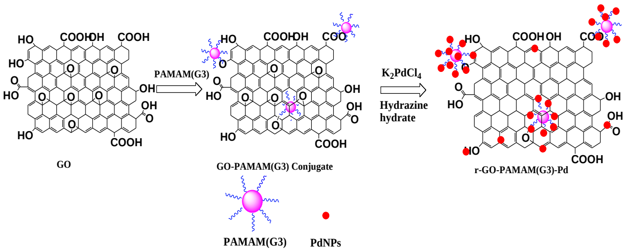

Scheme 1: Synthesis of r-GO-PAMAM (G3)-Pd composite.

Results and discussion

The graphene supported poly(amidoamine) dendrimer stabilized Pd nanoparticles (r-GO-PAMAM (G3)-Pd) composite was prepared as stated in the experimental procedure **(Scheme 1)**. The obtained composite was characterized with FT-IR, XRD, Raman, SEM and EDAX techniques.

FT-IR Analysis

FT-IR analysis was performed to investigate the structure and functional groups of the GO, PAMAM (G3) dendrimer grafted on GO conjugate & r-GO-PAMAM (G3)-Pd composite and the observed spectra were shown in **Fig. 1a., Fig.1b.** and **Fig.1c.** respectively. As noticed in **Fig. 1a,** the GO sheets exhibited characteristic absorption bands at 1723cm^{-1} and 1043 cm^{-1}, which attributed to C=O and C–OH stretching vibrations of the COOH group, respectively. The band at 1621cm^{-1} is assigned to the bending vibration of absorbed water molecules and the contributions of the sp^2(C=C) characteristics. Whereas, for the epoxy groups, a band at 1220 cm^{-1} can also be observed. The band at 3443 cm^{-1} can be ascribed to the stretching vibration of –OH. The presence of oxygen-containing functional groups such as C=O and C–O have further confirmed that the graphite indeed was oxidized into GO and was consistent with the literatures [27–28]. The presence of C=C groups showed that even graphite had been oxidized into GO and the main structure of layer graphite was still retained. Then, the amidation also confirmed by the characteristic peak at 3340.37 cm^{-1} due to stretching vibration of N-H group as shown in Fig.1b. Further, the two peaks noticed at 1358.76 cm^{-1} and 1067.97 cm^{-1} are corresponds to the bending vibration of N-H group. These peaks were due to condensation of surface amino groups of PAMAM (G3) dendrimer with –COOH groups of GO. This observation in turn confirmed the grafting of PAMAM (G3) dendrimer onto the surface of the GO. But in the case of r-GO-PAMAM (G3)-Pd **(Fig.1c.)** there is no characteristic peak appeared for N-H, this may be due to the Pd nanoparticle deposited on nitrogen.

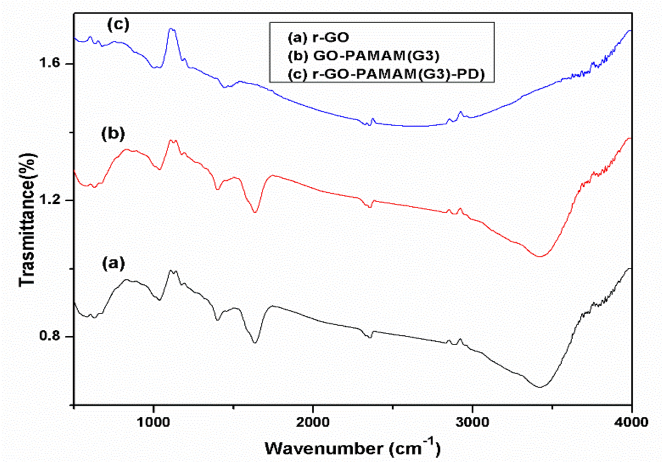

Fig.1. FT-IR spectra of (a) GO, (b) GO-PAMAM (G3) and (c) r-GO-PAMAM (G3)-Pd composite,

XRD analysis

XRD analysis was used to determine the average crystalline properties of the GO sheet & r-GO-PAMAM (G3)-Pd and the observed results were shown in **Fig. 2 (a)** and **Fig. 2 (b)** respectively. The prepared GO sheet showed a very strong peak at $2\theta = 25.2°$, which indicates that graphene oxide retains a layered structure but does not have a strict crystal lattice structure. The large interlayer distance is attributed to the formation of hydroxyl, epoxy, and carboxyl groups which increase the distance between the layers and this results agreed well with the literature values [29]. The diffraction peak (111) at around 35.88u in **Fig. 2 (b)** was found to shift slightly toward lower angles as compared with bulk Pd (40.12u, JCPDS 00–005-0681), indicating that the Pd-Pd interatomic distance increases after formation of the Pd NPs, which is consistent with a previous report [30–31].

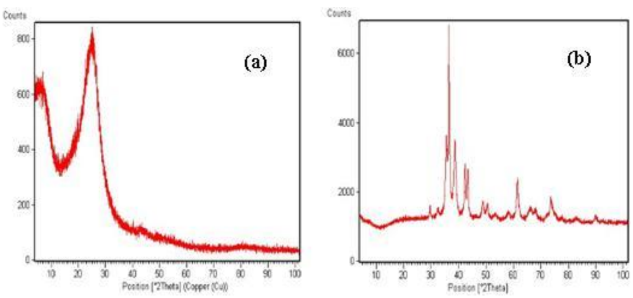

Fig.2. XRD spectra of (a) GO and (b) r-GO-PAMAM (G3)-Pd composite.

Raman spectroscopy

Raman spectroscopy is a non-destructive technique that is widely used to obtain structural information about carbon-based materials [32]. As shown in **Fig.3b.,** the spectrum of GO has shown two prominent peaks at 1353 and 1597 cm^{-1} which ascribed to D and G bands of graphene respectively. The G peak corresponds to the optical E_2g phonons at the Brillouin zone center resulting from the bond stretching of sp2 carbon pairs in both rings and chains. The D peak represents the breathing mode of aromatic rings arising due to the defect in the sample. The D-peak intensity is therefore often used as a measure for the degree of disorder [33]. It is generally known that the D to G-band intensity ratio (I_D/I_G) is an indication for the degree of defects/disorder occurred in graphite due to oxidation. The peak intensity ratio ((I_D/I_G)) obtained for GO is 1.2 which is higher than natural flake graphite ((I_D/I_G) = 0. 42) **(Fig.3a.),** and this value supports the oxidation of graphite. Raman spectrum of r-GO-PAMAM (G3)-Pd (Fig.3c.) also contains both D and G bands at 1353 and 1559 cm^{-1} respectively. The immobilization of Pd NPs on GO-PAMAM (G3) conjugate leads to shifted the G band to lower frequency (1559 cm^{-1}) and D-band frequency has not shifted, whereas its intensity increases. The peak intensity ratio ((I_D/I_G)) obtained for r-GO-PAMAM (G3)-Pd is 1.3 and this value proves increased defect/disorder, and this increased defect/disorder is due to more functionalization of dendrimer and followed by immobilization of Pd NPs.

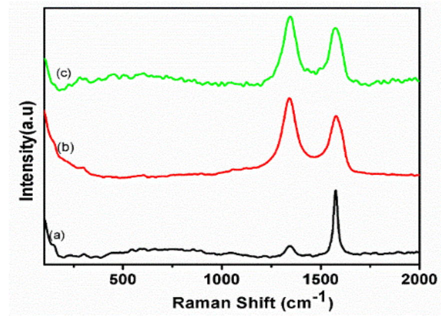

Fig.3. Raman spectra of (a) Graphite, (b) GO and (c) r-GO-PAMAM (G3)-Pd composite.

SEM and EDAX analyses

The SEM images of GO and r-GO-PAMAM (G3)-Pd composite were shown in **Fig.4a.** and **Fig.4b** respectively. On comparing SEM image of GO with graphite (Fig. S1), GO showed more exfoliated layered structure, which affords ultrathin and homogeneous graphene films. Such films are folded or continuous at times and it is possible to distinguish the edges of individual sheets, including kinked and wrinkled areas. However, after deposition of Pd NPs it shows heterogeneous and more intense aggregated bundles. Hence, this observation has strongly confirms that the palladium was deposited on the r-GO-PAMAM (G3) conjugate. Energy dispersive X-ray spectroscopy is used to identify and quantify the surface elements (semi-quantitatively). The percentage of elements in the composite viz. r-GO-PAMAM (G3)-Pd was established with EDAX analysis **(Fig.4c).** The EDAX spectrum r-GO-PAMAM (G3)-Pd composite shows the elements such as carbon, oxygen and palladium with the weight percentage of 42.59, 29.97and 27.44%, respectively and thus proves the functionalisation of PAMAM (G3) dendrimer with GO and immobilisation of Pd NPs.

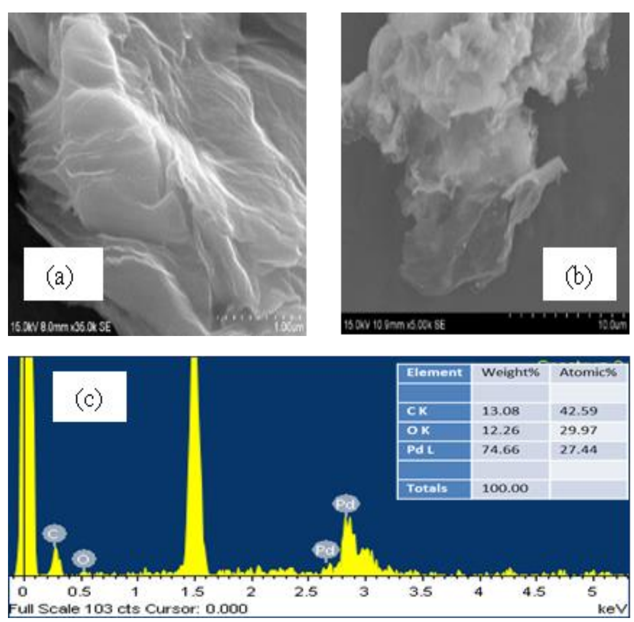

Fig.4. SEM images of (a) GO and (b) r-GO-PAMAM (G3)-Pd composite (c) EDAX analysis of r-GO-PAMAM (G3)-Pd composite.

Electrochemical study

The Electro-catalytic oxidation of FA was used as a model reaction to evaluate the potential of newly fabricated electrode namely viz. GC-r-GO-PAMAM (G3)-Pd electrode. The electro-catalytic behavior of fabricated composite electrode was evaluated with cyclic voltammetry and linear sweep voltammetry studies in 0.5 M H_2SO_4 as a blank at the potential range between -0.3 and 1.0 V and their corresponding results were given in **Fig. 6, Fig. 7a.** and **Fig. 7b** respectively. The typical cyclic voltammetry curve of GC-r-GO-PAMAM (G3)-Pd electrode in acid media (Fig.S2.) shows the characteristic features of Pd, including the well-defined hydrogen adsorption/desorption peaks noticed in the region of -0.2 V to -0.05 V [34], the oxidation of Pd observed at the positive potentials range between 0.50 to1.0V [35] and subsequent reduction of Pd oxide is noticed at 0.46V in the reverse scan. The CV results of GC-r-GO-PAMAM (G3)-Pd electrode in the solution containing 0.5 M H_2SO_4 and 0.5 M FA at a scan rate of 50 mVs^{-1} and effect of scan rates from 20, 40, 60, 80, 100 mVs^{-1} were shown in **Fig. 6 and Fig. 7a** respectively. As compared to the reported CV results of Pd/C [36], DNA-G-Pd and PVP-G-Pd, the prepared composite based electrode produced superior anodic peak potential. On comparing to the oxidation peak potential of HCOOH for r-GO-PAMAM (G3)-Pd composite with rGO-Pd, DNA-G-Pd and PVP-G-Pd, the oxidation peak potential of HCOOH is located at 0.15 V, which is 0.10 V more negative than that of DNA-G-Pd (0.25 V), 0.15 V more than Pd/C catalyst (0.3 V) and 0.50 V more than PVP-G-Pd catalyst (0.65 V). There is a systematic increase in anodic peak current (i_{pa}) against increase in the scan rate was observed for GC- r-GO-PAMAM (G3)-Pd electrode. Plot of i_{pa} vs square root of scan rate ($\upsilon^{1/2}$), result linear line with a slope value of 0.36 (Fig.S3.) suggesting that, the electron-transfer reaction are occurred via diffusion controlled [37]. This in turn indicating that electro-oxidation of HCOOH are strongly influenced by the size, morphology and dispersibility of Pd NPs and the properties of dendrimer [34]. It was evident that a peak associated with the FA oxidation process was observed in both forward and reverse scans.

Similarly, the observed LSV results shown in **Fig.7b.** The corresponding oxidation potentials of HCOOH on the r-GO-PAMAM (G3)-Pd composite are higher than GO/Pd. At 0.1 V, the GO/Pd shows a current density of 0.103 mA/cm^2 which is lower than r-GO-PAMAM (G3)-Pd composite (0.2 mA/cm^2). It is observed that the oxidation potential has been enhanced to the tune of 57%. All these results are strongly demonstrated that the r-GO-PAMAM (G3)-Pd composite based electrode are proved to be efficiently oxidized the HCOOH than the reported electro catalyst. This indicates that the functionalization of GO with dendrimer molecule has played effective role in entrapping more number of Pd NPs. That is, dendrimer provides abundant anchor sites, which would facilitate the formation of the uniform and monodisperse Pd NPs in well-defined binding sites along dendrimer surface. This in turn responsible for electrochemical active sites on the electrode surface and this reflected in effective electrochemical oxidation of FA.

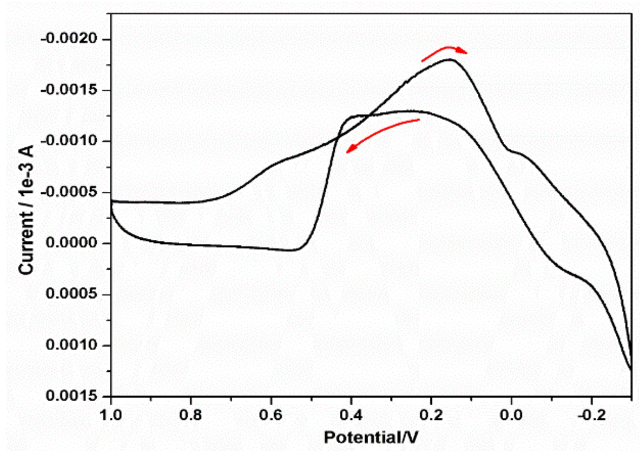

Fig. 6. Cyclic voltammogram of GC-r-GO-PAMAM (G3)-Pd electrode in 0.5 M H_2SO_4 +0.5 M HCOOH at a scan rate 50 mVs^{-1}.

Finally, r-GO-PAMAM (G3)-Pd composite follows different mechanism for FA oxidation then that of Pt catalyst. To account this effect for the oxidation of FA is as follows.

$$Pd(HCOOH)ads \rightarrow Pd(CO)ads + H_2O$$

$$Pd + H_2O \rightarrow Pd\ (OH)\ ads$$

$$Pd(OH)ads + Pd(CO)ads \rightarrow Pd + CO_2 + H^+$$

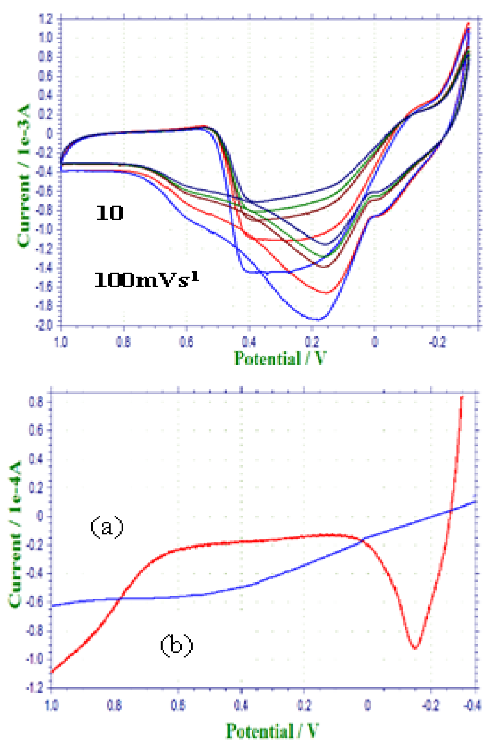

Fig.7. (a) Cyclic voltammograms of r-GO-PAMAM (G3)-Pd in 0.5 M H_2SO_4 +0.5 M HCOOH at different scan rates (b) Linear sweep voltammetry in 0.5 M H_2SO_4 + 0.5 M HCOOH solution at a scan rate of 50 mVs^{-1}.

The main reason for improved activity noticed in the composite electrode is due to the extensive affinity of Pd NPs towards the water molecules i.e., the ability of Pd NPs to activate water molecules at a lower potential than that on Pt and hence carbon monoxide (CO) was oxidized at lower potential. Hence, a significant improvement is noticed when Pd NPs has deposited on r-GO-PAMAM (G3) conjugate, which in turn initiate dissociative adsorption of H_2O and of FA. Thus it seems that the presence of Pd NPs limits the potential range of formation of poisoning species (adsorbed CO). At lower potential itself, the surface becomes free of adsorbed CO and then is able to re-adsorb FA molecules which can be available for further oxidization. Therefore, based on the observed results and explanations it is suggested that the GC-r-GO-PAMAM (G3)-Pd electrode has proved to be an effective oxidizer for FA especially at low potentials and the process is quasi reversible.

Conclusion

In summary, an electrochemically active graphene factionalized with poly(amidoamine) dendrimer stabilized Pd composite (r-GO-PAMAM-Pd) was prepared by simple and facile route and coated the same on GCE and then fabricated new efficient electrode viz., GC-r-GO-PAMAM-Pd. This stable and efficient electrode has successfully demonstrated for electro catalytic oxidation of HCOOH and the efficient of the electrode was established by measuring the peak potential through CV. The prepared electrode showed enhanced activity for FA electro-oxidation than with the Pd/GO, DNA-G-Pd and PVP-G-Pd hybrids. That is, GC-r-GO-PAMAM-Pd electrode is able to oxidize the HCOOH at the potential of 0.15V, whereas the rGO-Pd, DNA-G-Pd and PVP-G-Pd electrodes are able to oxidize the HCOOH at the potential 0.25 V, 0.3 V and 0.65 V. To best of our knowledge, as on now the newly fabricated electrode viz., GC-r-GO-PAMAM-Pd has proved to be supreme in FA electro-oxidation at lower potential. This is because of cooperative effect of GO, dendrimer and PdNPs. Since, dendrimer can chelate various transition metal cations, our work provides new insights into the design of novel catalytic materials based on graphene with full exploitation of their properties. Therefore, this electrode will be more efficient for fuel technologies application particularly for evolution of hydrogen at lower potentials.

Acknowledgements

The authors acknowledge DST under Purse Scheme (DST-PURSE-PHASE II), New Delhi, Government of India, for providing financial assistance. We also acknowledge National Centre for Nanoscience and Nanotechnology (NCNSNT), University of Madras for providing instrumentation facilities.

References

1. Winter, M.; Brodd, R.; *J. Chem. Rev.*, **2004**, 104, 4245-4269. **DOI:** 10.1021/cr020730k
2. Cheng, F.; Liang, J.; Tao, Z.; Chen, *J. Adv. Mater.*, **2011**, 23, 1695-1715. **DOI:** 10.1002/adma.201003587
3. Yu, X.; Pickup, P. *J. Power Sources.*, **2008**, 182, 124-132. **DOI:** 10.1016/j.jpowsour.2008.03.075
4. Uhm, S.; Lee, H. J.; Kwon, Y.; Lee, *J. Angew. Chem., Int. Ed.*, **2008**, 47, 10163-10166. **DOI:** 10.1039/c1cc11235j
5. Lee, H.; Habas, S. E.; Somorjai, G. A.; Yang, P. *J. Am. Chem. Soc.*,**2008**, 130, 5406-5407. **DOI:** 10.1021/ja800656y
6. Zhang, S.; Shao, Y.; Yin, G.; Lin, Y. *Angew. Chem., Int. Ed.*, **2010**, 49, 2211-2214. **DOI:** 10.1002/anie.200906987
7. Antolini, E.; *Energy Environ. Sci.*, **2009**, 2, 915-931. **DOI:** 10.1039/B820837A
8. Lu, L.; Li, H.; Hong, Y.; Luo, Y.; Tang, Y. ; Lu, T.; *J. Power Sources.*, **2012**, 210, 154-157. **DOI:** 10.1016/j.jpowsour.2012.03.010
9. Cheng, N.;Lv, H.; Wang, W.; Mu, S.; Pan, M.; Marken, F.; *J. Power Sources.*, **2010,** 195,7246-7249. **DOI:** 10.1016/j.jpowsour.2010.05.039
10. Mazumder, V.; Sun, S. *J. Am. Chem. Soc.*, **2009**, 131, 4588-4589. **DOI:** 10.1021/ja9004915
11. Jiujun, Z. (Eds.); PEM Fuel Cell Electrocatalysts and Catalyst Layers: Fundamentals and Applications; Springer Science & Business Media, **2008**. **DOI:** 978-1-84800-936-3
12. Wang, L.; Nemoto, Y.; Yamauchi, Y.; *J. Am. Chem. Soc.*, **2011**,133, 9674-9677. **DOI:** 10.1021/ja202655j
13. Novoselov, K. S.; Geim, A. K.; Morozov, S. V.; Jiang, D.; Zhang,Y.; Dubonos, S. V.; Grigorieva, I. V.; Firsov, A.;*A. Science*., **2004**, 306,666−669. **DOI:** 10.1126/science.1102896
14. Venkateswara Rao, C.; Cabrera, C.R.; Ishikawa, Y.;*J. Phys. Chem. C.*, **2011,**115, 21963-21970. **DOI:** 10.1021/jp202561n
15. Rao, C.N.R.; Sood, A.K.; Subrahmanyam, K.S.; Govindaraj, A.; *Angew. Chem. Int. Ed.*, **2009**, 48, 7752-7777. **DOI:** 10.1002/anie.200901678
16. Hassan, H. M. A.; Abdelsayed, V.; Khder, A. E. R. S.; AbouZeid,K. M.; Terner, J.; El-Shall, M. S.; Al-Resayes, S. I.; El-Azhary, A. A.; *J.Mater. Chem.*, **2009**, 19, 3832-3837. **DOI:** 10.1039/B906253J
17. Muszynski, R.; Seger, B.; Kamat, P. V.;*J. Phys. Chem. C.*, **2008**,112, 5263-5266. **DOI:** 10.1021/jp800977b
18. Chen, X. M.; Wu, G. H.; Chen, J. M.; Chen, X.; Xie, Z. X.;Wang, X. R.; *J. Am. Chem. Soc.*, **2011**, 133, 3693-3695. **DOI:** 10.1021/ja110313d
19. Li, Y.; Fan, X.; Qi, J.; Ji, J.; Wang, S.; Zhang, G.; Zhang, F.;*NanoRes.*, **2010**, 3, 429-437. **DOI:** 10.1007/s12274-010-0002-z
20. Chen, X. M.; Wu, G. H.; Chen, J. M.; Chen, X.; Xie, Z. X.; Wang, X. R.; *J. Am. Chem. Soc.*, **2011**, 133, 3693-3695. **DOI:** 10.1021/ja110313d
21. Pileni, M. P.; *Nat. Mater.*, **2003**, 2, 145-150. **DOI:** 10.1038/nmat817
22. Fu, B. S.; Missaghi, M. N.; Downing, C. M.; Kung, M. C.; Kung, H. H.; Xiao, G. M.;*Chem. Mater.*, **2010**, 22, 2181-2183. **DOI:** 10.1021/cm100159j
23. Newkome, G.R.; Shreiner, C.D.; *Polymer.*, **2008**, 49, 1-173. **DOI:** 10.1016/j.polymer.2007.10.021
24. Murugan, E.; Vimala, G.; *J. Colloid Interface Sci.*, **2011**, 357(2), 354-365. **DOI:** 10.1016/j.jcis.2011.02.009
25. Paulchamy, B.;, Arthi, G.; Lignesh, BD.; *J Nanomed Nanotechnol*., **2015** 6, 253. **DOI:** 10.4172/2157-7439.1000253
26. Murugan, E.; Sivaranjani, A.; *RSC Adv*., **2014**, 4, 35428-35441. **DOI:** 10.1039/C4RA04646C
27. Zhou, Y.; Zhu, X.; Yang, X.; Jiang.; *New Journal of Chemistry.*, **2011**, 35(2), 353-359. **DOI:** 10.1039/c0nj00623h
28. Zhang, Y.; Pan, C.; *Journal of Materials Science*., **2011**, 46(8), 2622-2626. **DOI:** 10.1007/s10853-010-5116-x

29. Marcano, D. C.; Kosynkin, D. V.; Berlin, J. M.; *ACS Nano.*, **2010**, 4(8), 4806-4814.
DOI: 10.1021/nn1006368
30. Piao, Y.; *Small*., **2007**, 3, 255-260.
DOI: 10.1002/smll.200600402
31. Li, C.; *Angew. Chem. Int. Ed.*, **2009**, 48, 6883-6887.
DOI: 10.1002/ange.200902786
32. Ferrari, A. C.; Robertson, J.; *Phys. Rev. B.*, **2000**, 61, 14095-14107.
DOI: 0163-1829/2000/61~20!/14095~13
33. Tuinstra, F.; Koenig, J. L.; *J. Chem. Phys.*, **1970**, 53, 1126-1130.
DOI: 10.1063/1.1674108
34. Qu, K.; Wu, L.; Ren, J.; Qu, X.; *ACS Appl. Mater. Interfaces.*, **2012**, 4, 5001-5009.
DOI: 10.1021/am301376m
35. Hosseini, H.; Mahyari, M.; Bagheri, A.; Shaabani, A.; *Journal of Power Sources*., **2014**, 247, 70-77.
DOI: 10.1016/j.jpowsour.2013.08.061
36. Chen, X.; Wu, G.; Chen, J.; Chen, X.; Xie, Z.; Wang, X.; *J. Am. Chem. Soc.*, **2011**, 133, 3693–3695.
DOI: 10.1021/ja110313d
37. Batchelor-McAuley, C.; Luı´s, A.; Goncalves, M.; Xiong, L.; Barrosb, AA.; Compton, RG.; *Chem. Commun.*, **2010**, 46, 9037–9039.
DOI: 10.1039/C0CC03961F

